Review

Check for updates

Recycling Bayer and sintering red muds in brick production: a review

Yu-jia XIAO[1], Michelle TIONG[1], Kim Hung MO[2], Ming-zhi GUO[3], Tung-chai LING[1]✉

[1]*College of Civil Engineering, Hunan University, Changsha 410082, China*
[2]*Department of Civil Engineering, Faculty of Engineering, Universiti Malaya, Kuala Lumpur 50603, Malaysia*
[3]*College of Mechanics and Materials, Hohai University, Nanjing 210098, China*

Abstract: Red mud (RM) is a solid waste generated from the extraction of alumina from bauxite. It is estimated that more than 1.5 billion tonnes of RM are produced annually worldwide. Stockpiling and landfilling of RM is toxic for the environment due to the presence of high quantities of alkali-generating minerals and metal ions. The high cost of RM treatment and limited land availability encourage the recycling and reuse of RM as construction materials. In many developing countries, brick remains the ubiquitous building material. Thus, it is reasonable to use brick as a medium to accommodate a large amount of RM. In this review, the properties of RM are analyzed and their applications in bricks are discussed. Two common types of RM, namely Bayer red mud (BRM) and sintering red mud (SRM), are introduced along with the methods to produce bricks from them through firing, cementing, and geopolymerization. High alkaline-based BRM is particularly useful as a raw material to produce fired brick and geopolymer brick, whereas SRM, which contains more dicalcium silicate (C_2S) and some cementitious phases, can be favorably used to produce cementing brick. RM geopolymer brick normally has more strength (up to 51 MPa) than fired and cementing bricks, and good durability (no efflorescence) with low energy consumption and CO_2 emissions. Finally, several solutions have been suggested to resolve the issue of the radioactivity of RM brick, and strict regulation of its application has been imposed in some countries, such as China.

Key words: Bauxite residue; Red mud (RM); Firing brick; Cementing brick; Geopolymer brick; Construction materials

1 Introduction

Red mud (RM) (or bauxite residue) is a solid waste generated from alumina production with a total annual global production exceeding 120 million tonnes (Power et al., 2011). Usually, RM is stockpiled in landfills. This disposal practice causes great concern for the surrounding environment because RM has high alkalinity and contains heavy metals, which are harmful to the water, soil, groundwater, and air of the surrounding area (Liu et al., 2009b; Sutar et al., 2014).

For better environmental protection and sustainable development, many researchers have studied treatments and uses of RM, including valuable metal recovery, preparation of construction materials, and as an absorbent for wastes or a catalyst in diverse processes. Among these applications, recycling of RM in building and construction materials appears to be a promising option to consume a large volume of RM. RM has been widely used for the production of cement clinker and various construction products, such as mortar, concrete, glass-ceramics, block, brick, and ceramics (Liu et al., 2009b; Liu and Zhang, 2013; Khairul et al., 2019).

Since bricks have been a major construction and building material in many developing countries and are still in high demand, using RM to produce bricks is highly desirable. Usually, conventional bricks require natural resources like sand or gravel and clay as raw materials. RM can be a suitable alternative to clay due to its similar characteristics. For example, the presence of 4%−5% of alkali can provide good fluxing action, resulting in good plasticity and good bonding (Samal et al., 2013). Extensive studies have been published on the use of RM in bricks. However, a systematic review of different methods for processing RM and their effects on producing different types of brick is lacking.

In this review, we present an overview of the state-of-the-art use of different types of RM (i.e., Bayer and sintering) and the various methods (i.e., firing, geopolymerization, and cementing) used to produce bricks. Their advantages and disadvantages are discussed in detail to allow a better understanding of their applications in construction. The existing problems and future research need in response to major durability concerns are also highlighted.

2 Types of red muds: production processes and properties

RM is a by-product of alumina production, in which the bulk of bauxite sources is used as a feed for the manufacture of alumina. There are two types of production process, the Bayer process and the sintering process, which are defined according to the chemical nature of the bauxite sources (Liu et al., 2009b; Liu and Wu, 2012). Fig. 1 shows the production processes of these two approaches (Klauber et al., 2011), and Fig. 2 shows the morphology of RM produced by each process (Zhang et al., 2018).
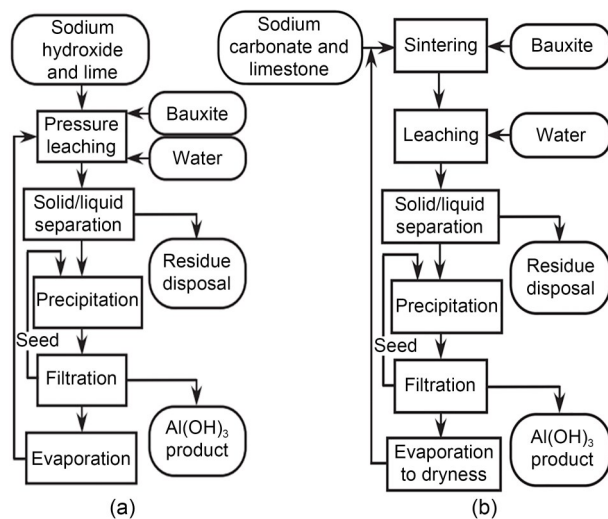

Fig. 1 Production processes of alumina: (a) Bayer process; (b) sintering process. Reprinted from (Klauber et al., 2011), Copyright 2011, with permission from Elsevier

2.1 Bayer production process and its properties

Normally, the Bayer process is applied to aluminum-bearing minerals in high-grade bauxite sources such as gibbsite ($Al(OH)_3$), boehmite (γ-AlO(OH)), and
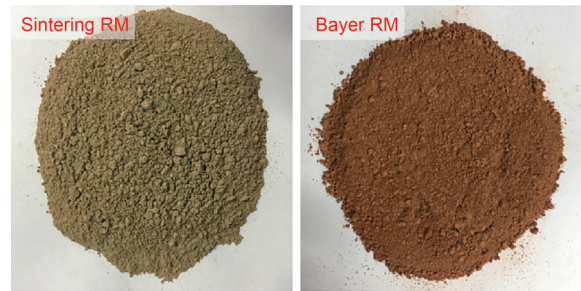

Fig. 2 Morphology of RM produced from sintering and Bayer processes. Reprinted from (Zhang et al., 2018), Copyright 2018, with permission from Elsevier

diaspore (α-AlO(OH)). These minerals are selectively extracted from the insoluble components (mostly oxides) by dissolving them in a solution of sodium hydroxide (NaOH), lime, and water at 140–280 °C and 3.5-MPa pressure (Liu et al., 2009b; Sutar et al., 2014). A sodium aluminate ($NaAlO_2$) supersaturated solution or 'pregnant liquor' is obtained by the pressure leaching step. The general chemical reactions in the Bayer process are given in the following equations.

For gibbsite (at 140 °C),

$$Al(OH)_3 + Na^+ + OH^- \rightarrow Al(OH)_4^- + Na^+. \quad (1)$$
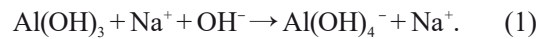
For boehmite and diaspore (at 200–280 °C),

$$AlO(OH) + Na^+ + OH^- + H_2O \rightarrow Al(OH)_4^- + Na^+. \quad (2)$$

After that, the solid/liquid separation of 'pregnant liquor' is carried out. The solid phase, namely the RM, is treated as waste residue, while the liquid phase then undergoes precipitation, filtration, and evaporation to obtain aluminum hydroxide ($Al(OH)_3$) (Kelessidis et al., 2007) (Fig. 1).
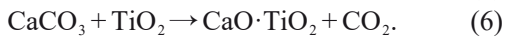
RM that undergoes the Bayer production process is known as Bayer red mud (BRM). Fe_2O_3 and Al_2O_3 are the major components in BRM due to a higher Fe_2O_3 content in the bauxite sources and the low efficiency of the Bayer process (Klauber et al., 2011). In general, the main mineralogical phases of BRM are gibbsite ($Al(OH)_3$), boehmite (γ-AlOOH), hematite (Fe_2O_3), goethite (FeO(OH)), quartz (SiO_2), anatase (TiO_2), rutile (TiO_2), calcite ($CaCO_3$), dolomite ($CaMg(CO_3)_2$), hydrogarnet ($Ca_3Al_2(SiO_4)_2(OH)_4$), sodalite ($Na_8(Al_6Si_6O_{24})Cl_2$), anhydrite ($CaSO_4$), and cancrinite ($Na_6Ca_2(CO_3)_2Al_6Si_6O_{24}\cdot 2H_2O$) (Yang et al., 2006; Sutar et al., 2014; Sun et al., 2019). Usually,

the particle size of BRM falls within the range of 3–10 μm (Han et al., 2011), and depends heavily on the degree of grinding of the bauxite (Sutar et al., 2014).

Various modifications to the standard Bayer process have been attempted to reduce the high silica levels and some bauxite ores, and improve the alumina production efficiency (Yang, 1993; Meyer, 2004; Bi, 2006; Liu et al., 2009b). On the other hand, low grade bauxite containing 8%–15% reactive silica can be treated by a sintering process at high temperatures.

2.2 Sintering production process and its properties

In the sintering process (Fig. 1), low-grade bauxite is commonly sintered with limestone and soda ash at about 1200 °C in rotary sintering kilns to form sodium aluminate ($Na_2O·Al_2O_3$), calcium silicate ($CaO·SiO_2$), sodium ferrite ($Na_2O·Fe_2O_3$), and calcium titanate ($CaO·TiO_2$) (Liu et al., 2009b). The major reactions are listed as follows:

$$Na_2CO_3 + Al_2O_3 \rightarrow Na_2O·Al_2O_3 + CO_2, \quad (3)$$
$$CaCO_3 + SiO_2 \rightarrow CaO·SiO_2 + CO_2, \quad (4)$$
$$Na_2CO_3 + Fe_2O_3 \rightarrow Na_2O·Fe_2O_3 + CO_2, \quad (5)$$
$$CaCO_3 + TiO_2 \rightarrow CaO·TiO_2 + CO_2. \quad (6)$$
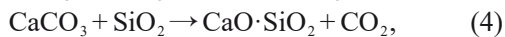
After sintering, water leaching of the sintered residue associated with RM occurs, followed by the carbonation of the resulting liquor to precipitate aluminum hydroxide ($Al(OH)_3$), which is then used to produce alumina. The phase separation and treatment are similar to those of the Bayer process. However, the sintering process requires a higher temperature to fire the bauxite so that the alumina-containing minerals can be effectively broken down and rendered into a soluble form of sodium aluminate. Therefore, the sintering process is relatively energy- and capital-intensive, as well as less environmentally-friendly (Klauber et al., 2011).

For sintering red mud (SRM), SiO_2 and CaO are the major oxides, while the main mineralogical constituents are β-$2CaO·SiO_2$, calcite ($CaCO_3$), aragonite ($CaCO_3$), hematite (Fe_2O_3), gibbsite ($Al(OH)_3$), and perovskite ($CaTiO_3$) (Yang et al., 2006; Sutar et al., 2014). This is why SRM is dull grey in colour, while BRM is usually dark red (Zhang et al., 2018). Due to $CaCO_3$ and SiO_2 precipitation and crystallization during the sintering process, the particle size of SRM usually falls within the range of 1–20 μm, which is

expected to be larger than that of BRM (Han et al., 2011).

2.3 Comparison of red muds from the Bayer and sintering processes

The properties and characteristics of RMs can vary depending on the different bauxite resources and alumina production processes. The chemical compositions of RMs used for brick production are listed in Table 1, and the basic properties of both SRM and BRM in Table 2.

Because RM derived from different sources and treatment methods varies considerably in its chemical and mineral contents, specific methods (e.g., firing, cementing, and geopolymerization) should be tailored for each type of RM to fabricate bricks. The effects of different RMs on the production of bricks by different methods of firing, cementing, and geopolymerization are discussed in the following section.

3 Producing brick from Bayer red mud

3.1 Production of fired brick

Fired bricks require molding and high temperature baking, and commonly have high strength. They have been applied mainly in masonry bearing and non-bearing walls. Clay is the major raw material to produce fired bricks. Compared with clay, BRM has less silica but more alumina and fluxing oxides, making it perfect for combination with clay to manufacture bricks with less open porosity and a more vitrified structure (Rehman et al., 2020). Moreover, the high alkaline oxide content of BRM makes it a suitable material for the production of fired bricks due to the stabilization of soluble sodium during firing (Kalkan, 2006; Samal et al., 2013). Table 3 lists previous published studies regarding BRM fired bricks.

Sglavo et al. (2000a) pointed out that when the temperature is increased up to 900 °C, BRM experiences a loss of H_2O and an accompanying release of CO_2. This gives rise to the red colour appearance and the extremely fine particle size of BRM. Meanwhile, nepheline and $Na_2Si_2O_5$ are formed at higher temperatures. A ceramic body (a kind of fired building material) with BRM achieves 20-MPa flexural strength and <40% porosity with a 102-nm average pore radius. Rai et al. (2013) proposed that BRM fired at 1200 °C

Table 1 Chemical compositions of BRM and SRM within bricks

Type of RM	Chemical composition (in weight) (%)								Reference
	SiO_2	Al_2O_3	Fe_2O_3	CaO	Na_2O	MgO	TiO_2	LOI[*] (%)	
BRM	4.48	11.75	47.16	5.45	4.57	1.82	6.79	13.90	Youssef et al. (2001)
	5.70	12.20	35.50	7.90	4.60	–	15.20	–	Mymrin et al. (2003)
	13.50	20.20	35.04	5.30	9.40	0.33	4.00	8.44	Kavas (2006)
	20.98	22.00	27.93	6.23	10.50	1.32	2.30	9.96	Liu et al. (2009a)
	3.13	22.08	38.41	1.05	5.84	–	4.56	24.20	Annan et al. (2012)
	9.20	15.16	49.91	2.80	3.98	–	3.82	–	Kumar (2015)
	8.80	18.20	33.10	4.70	3.80	0.09	19.60	–	Mandal and Sinha (2017)
	24.10	44.74	14.14	1.16	5.48	0.09	5.90	–	Mandal et al. (2017)
	12.04	13.30	53.21	5.98	5.16	–	5.48	4.20	Shoppert et al. (2019)
	22.50	25.30	8.10	15.10	8.80	1.30	3.80	12.10	Sun et al. (2019)
	16.70	20.40	23.70	13.60	8.00	0.40	4.90	11.20	Sun et al. (2019)
	16.60	23.80	30.60	2.20	9.70	0.20	6.90	9.10	Sun et al. (2019)
	15.30	20.50	21.20	14.50	8.10	0.70	5.70	12.50	Sun et al. (2019)
	16.40	19.10	22.00	16.00	7.60	0.90	5.00	12.00	Sun et al. (2019)
	14.30	28.10	34.90	5.20	9.80	0.00	7.70	0.00	Kim et al. (2019)
	4.87	18.08	50.89	1.13	3.45	0.07	9.33	10.26	Arroyo et al. (2020)
SRM	17.78	6.27	12.32	37.52	2.75	1.15	3.27	17.76	Zhang et al. (2011)
	23.72	23.24	9.90	18.25	3.68	1.89	3.29	14.16	Lv et al. (2013)
	18.00	10.00	12.60	42.60	2.68	0.90	4.60	–	Fu and Xiong (2014)
	35.31	8.46	8.28	29.86	3.16	3.42	–	9.27	Ma et al. (2014)
	15.39	17.70	9.55	32.55	1.20	2.57	4.47	–	Feng et al. (2015)
	21.28	6.96	12.29	39.82	1.73	2.41	3.39	11.20	Liu et al. (2017b)
	8.71	11.80	36.90	23.80	0.27	1.01	3.54	12.46	Zinoveev et al. (2019)
	6.18	9.32	30.78	12.18	5.57	0.17	5.92	–	Mi et al. (2021)

[*]LOI: loss on ignition; LOI=$(G_1-G_2)/G_1 \times 100\%$; G_1: weight before ignition; G_2: weight after ignition

Table 2 Comparison of basic properties of SRM and BRM

Type of RM	Main chemical constituents	Mineralogical constituents	Particle size (μm)
SRM	SiO_2, CaO	β-2CaO·SiO_2, calcite ($CaCO_3$), aragonite ($CaCO_3$), hematite (Fe_2O_3), gibbsite ($Al(OH)_3$), and perovskite ($CaTiO_3$)	1–20
BRM	Fe_2O_3, Al_2O_3	Gibbsite ($Al(OH)_3$), boehmite (γ-AlOOH), hematite (Fe_2O_3), goethite (FeO(OH)), quartz (SiO_2), anatase (TiO_2), rutile (TiO_2), calcite ($CaCO_3$), dolomite ($CaMg(CO_3)_2$), hydrogarnet ($Ca_3Al_2(SiO_4)_2(OH)_4$), sodalite ($Na_8(Al_6Si_6O_{24})Cl_2$), anhydrite ($CaSO_4$), and cancrinite ($Na_6Ca_2(CO_3)_2Al_6Si_6O_{24}·2H_2O$)	3–10

had a lower pH (within the permissible limit of 8.4), effectively tackling the caustic soda problem. Thus, BRM can be used as an alternative to clay for brick production with no efflorescence. Alekseev et al. (2019) found that in fired bricks containing 50%–100% BRM, there were strong cohesive forces between the clay and BRM particles, associated with the formation of a glassy phase at much lower temperatures (900–1150 °C), resulting in better mechanical properties than those of normal fired bricks.

To improve the performance of fired bricks, researchers have combined industry wastes such as fly ash, boron waste, and gold tailings with BRM. Singh et al. (2014) observed that a mixture of 40% BRM

Table 3 Studies on the production of bricks from red mud by firing

No.	Reference	Raw material	Ratio of RM (%)	Brick forming process (including pretreatment)	Characteristic				
					Density (g/cm³)	Water absorption (%)	Porosity (%)	Strength	Other
1	Sglavo et al. (2000a, 2000b)	RM, clay	0–50	Dried RM at 120 °C for 2 h; Milled clays A and B into powders with particle sizes lower than 100 mm; Mixed clay A with 0–50% RM, and clay B with 0–20% RM; Pressed samples at 10 MPa or slip casting; Sintered RM and clay A at 850 °C, and RM and clay B at 950 and 1050 °C for 15 min	1.0–1.8		~40	5–20 MPa (flexural strength)	10^2–10^3 nm average pore radius
2	Kavas (2006)	RM, clay, fine wastes (boron wastes)	85–95	Ground and preheated at 100 °C; Added water and pressed slurry in 50 mm×12 mm×8 mm; Firing specimens at 700, 800, and 900 °C for 1 h; Cooled down to an ambient temperature		8.3–9.5		9 MPa (bending), 300 MPa (compressive strength)	4.5% drying and 1.2% firing shrinkage
3	Annan et al. (2012)	RM, clay	40–90	Milled RM with particle size less than 100 µm; Digested RM with 2-mol/L NaOH at 135–150 °C; Dried residue at 110 °C for 48 h; Mixed raw materials; Produced bricks with 6 cm×3 cm×2 cm; Firing at temperatures 800–1100 °C at 5 °C/min for 5 h	1.3–1.8	0.16–0.32	0.25–0.50 (apparent porosity)	3.2–12.5 MPa	
4	Rai et al. (2013)	RM, fly ash	25–75	Mixed RM, fly ash, and water; Sintered mixtures, cooled and added 100-mL distilled water; Pressed mixtures at 200 kg/cm²; Dried samples overnight at 110 °C; Sintered samples at 1200 °C for 2 h	1.47–1.51	24		31.70–134.18 kg/cm²	None efflorescence
5	Singh et al. (2014)	RM, fly ash, rice husk, saw dust, polystyrene	0–100	Mixed RM, fly ash, saw dust, and water; Prepared, dried samples for 48 h in air; Followed by oven at 110–120 °C for 24 h; Harden samples at 1000–1200 °C	1.5		40–60	160 MPa (compression strength)	
6	Singh and Jawaid (2015)	RM, soil (clay)	50–70	Mixed RM and soil; Pressed mixtures in three equal layers, each layer being given 25 blows of the 2.5-kg rammer dropped from a height of 30 cm; Maintained samples in the natural conditions	1.55–1.69			3.5–7.6 N/mm²	23–30 g/cm³ moisture content
7	Liu et al. (2017a)	RM, SiO₂	~63	Dried and ground RM and SiO₂; Mixed raw materials, pressed mixtures at 5 MPa and dried; Sintered samples at 1100, 1125, 1150, and 1175 °C; Cooled down to an ambient temperature	1.68		47.12	22.69 MPa (compressive strength)	7.29% linear shrinkage

To be continued

Table 3 (continued)

No.	Reference	Raw material	Ratio of RM (%)	Brick forming process (including pretreatment)	Density (g/cm³)	Water absorption (%)	Characteristic			
							Porosity (%)	Strength	Other	
8	Mandal et al. (2017)	RM, fly ash, sawdust	0–100	Dried RM and fly ash; Mixed raw materials; Extruded into a 30 mm×30 mm×30 mm adobe with 15 MPa; Heated to 110 °C and kept for 2 h; Fired at 1000, 1100, and 1200 °C at 5 °C/min for 2 h	1.0		60	20 MPa (cold crushing strength)		
9	Scribot et al. (2018)	RM, clay	0–30	Modified RM after dewatering treatment; Dried and ground RM; Added water, mixed and compacted ceramic specimens; Fired specimens at 950 and 1015 °C for 2 h	1.9	10.8–15.7		19.1 MPa (flexural strength),73 MPa (compression strength)	5% shrinkage	
10	Kim et al. (2019)	RM, gold tailing, chemical materials	20–80	Mixed RM and gold tailing; Added five chemical materials under pressure and stirred mixture; Frozen slurry mixture at 253 K for 24 h and thawed at 293 K; Heated slurry gel at 333 K for 3 d; Sintered sample at 773 K for 2 h, and at 1523 K for 30 min	0.5–0.8		75		0.1–0.2 W/(m·K) thermal conductivity	
11	Alekseev et al. (2019)	RM, spent-foundry sand	50–100	Mixed raw materials and water; Compacted mixtures at 5 MPa; Dried samples at 100 °C; Burned samples for 3 h at 800, 900, 1000, 1050, 1100, 1150, 1200, and 1225 °C	1.65–2.07	2.77–14.41		10.54 MPa (flexural strength)	6.62%–7.92% shrinkage	
12	Arroyo et al. (2020)	RM, natural clay	0–80	Mixed RM and natural clay for 4 min; Deposited mixtures in cylindrical molds; Pressurized mixtures (5 MPa) for 5 min, molding pressure 4–50 MPa; Cured samples at 298 K for 48 h, then dried at 378 K for 48 h more; Heated samples from 298 to 773 K at 100 K/h, from 773 to 1373 K at 50 K/h, and maintaining for 8 h	1.5–2.0	12–35		16 MPa		
13	Babisk et al. (2020)	RM, yellow clay, green clay	33–100	Dried and sieved raw materials; Added water and milled mixtures; Compacted mixtures at 120 mm×30 mm× 12 mm under 20 MPa; Sintered samples at 850, 950, and 1050 °C for 2 h with 2 °C/min	2.69–3.03	15–35		4–13 MPa	1.0%–5.5% shrinkage	

and 60% fly ash fired at 1200 °C can produce excellent fired lightweight foam bricks with a compressive strength of 160 MPa, 48% porosity, and 1500-kg/m^3 bulk density. Kavas (2006) found that adding 15% boron waste as a fluxing agent can enable the firing temperature to be reduced to 700 °C and produce fired clay-BRM bricks with a compressive strength of about 300 MPa and bending strength of 10 MPa. Kim et al. (2019) discovered that adding 40% gold tailings to the fired BRM brick without clay can increase the thermal conductivity by 0.2 W/(m·K). They further produced a fired foam brick by adopting a new slurry gelation and foaming method, obtaining a brick with over 75% porosity within 30 min. Moreover, the addition of gold tailings can increase the pore diameter and produce a closed pore structure. Hence, there is high potential to use different industrial wastes in combination with BRM to produce competitive fired bricks.

Different pre-treatment methods of raw materials have been adopted to improve the performance of BRM bricks, such as adding alkaline or using different brick forming methods (e.g., slip casting and pressing mixtures in three equal layers) (Table 3). Using slip casting can produce fired bricks with low shrinkage upon drying (Sglavo et al., 2000a, 2000b). Singh and Jawaid (2015) developed a new forming brick technique: each layer was given 25 blows from a 2.5-kg rammer dropped from a height of 30 cm, with a total of three layers formed. The produced fired BRM bricks showed better mechanical properties, fire retardancy, and abrasive wear resistance than ordinary bricks. The presence of 4%–5% alkali in BRM provides good fluxing action, which contributes to better plasticity and bonding in fired BRM bricks. Pretreatment of BRM is important to improve the efficiency of brick manufacturing and reduce energy consumption and environmental pollution during the brick firing process. For example, prior to brick manufacture, dissolving BRM at 135–150 °C and drying at 110 °C for 48 h can reduce the firing temperature to 800, 950, or 1100 °C compared to that of normal fired brick (1150 °C). This is because pretreatment can remove the moisture from the fired brick, allowing more uniform heating (Singh et al., 2014; Mandal et al., 2017; Alekseev et al., 2019). Annan et al. (2012) obtained BRM fired bricks with a bulk density of 1.3–1.8 g/cm^3 and compressive strength of 3.2–12.5 MPa, meeting the standard brick requirement. In addition,

certain burning conditions, such as controlled firing time and temperature, can enhance the performance of the produced brick. For example, Kim et al. (2019) froze the slurry mixture at −20 °C for 24 h, followed by thawing at 20 °C and heating the slurry gel at 60 °C for 3 d. After that, the samples were sintered, first at 500 °C for 2 h, and finally at 1250 °C for 30 min. Arroyo et al. (2020) cured brick samples at 25 °C for 48 h, then dried them at 105 °C for 48 h. Afterwards, the samples were heated from 25 to 500 °C at 100 °C/h and then from 500 to 1100 °C at 50 °C/h, and then maintained at 1100 °C for 8 h. The resulting bricks had a density of 1.5–2.0 g/cm^3, water absorption of 12%–35%, and compressive strength of 16 MPa with no environmental risk. Overall, by conducting pre-treatments and adopting appropriate forming methods to produce BRM fired bricks, a better performance and more eco-friendly process can be expected due to the lower firing time and temperature.

3.2 Production of cementing brick

Cementing brick does not need kiln firing, but relies on the cementing properties of the incorporated materials. Cement, gypsum, and lime are usually needed for the development of mechanical strength through the formation of calcium silicate hydrate (C-S-H). BRM has a low cementitious property, and its application in cementing brick is therefore limited.

Table 4 lists the few studies using BRM in cementing brick. In most studies, up to 70% BRM was used with the addition of a small amount of cement, fly ash, and lime. Mymrin et al. (2003) used BRM and waste ferrous slag as raw materials to prepare cementing brick, which met the required strength of 11 MPa. Liu et al. (2009a) prepared low-iron (Fe) BRM upon recovery of Fe from BRM. They noticed that the prepared cementing brick incorporated with the low-iron (Fe) BRM yielded higher strength (24.1 MPa) and was more environmentally friendly than ordinary cementing brick. Xu et al. (2019) combined BRM with fly ash as key ingredients for making cementing brick and found that with a CaO/SiO$_2$ mass ratio of 1.23, the optimal mechanical strength (32 MPa) and water resistance (softening coefficient greater than 0.8) were achieved. They explained that the improved performance was associated with the growth of amorphous gel compounds from BRM, and wastes (slag and fly ash)

Table 4 Summary of BRM in cementing brick

No.	Reference	Raw material	Ratio of RM (%)	Brick forming process (including pretreatment)	Characteristic			
					Density (g/cm³)	Water absorption (%)	Strength (MPa)	Other
1	Mymrin et al. (2003)	RM, ferrous slag, CaO or Portland cement	70	Mixed raw materials with water; Pressed mixtures at 10 MPa; Harden samples at 98% humidity			6.3–11.0	2.35% shrinkage
2	Liu et al. (2009a)	RM, slaked lime	80–100	Mixed RM after magnetic separation and slaked lime; Pressed mixtures at 20 MPa; Cured samples with steam of 80 °C under 1 atm for 11 h			24.1 (compression strength)	
3	Fang (2010)	RM, cement, sand	20–80	Dry and milled BRM; Mixed raw materials and water; Molded mixtures in 2 cm×20 cm×10 cm; Cured samples at 24 °C and 60% humidity for 24 h			40–90 (compression strength)	Severe efflorescence
4	Mandal and Sinha (2017)	RM, bottom ash, lime, gypsum	0–85	Prepared slurry in lime and gypsum; Mixed slurry in a dry mixture of bottom ash and RM; Molded mixtures in 30 mm cubic shape at 15 MPa; Dried for 2 d at room temperature (27–29 °C); Cured samples in a water curing tank for 7, 14, 21, and 28 d	1.950	19.5	7.56 (crushing strength)	
5	Xu et al. (2019)	RM, fly ash, cement, aggregate		Mixed RM and water; Added fly ash and cement; Added aggregate and mixed for 2–3 min; Pressed at 5 MPa for 30 s; Cured samples at 20 °C, a relative humidity of 95% for 3, 7, and 28 d	2.01	19.9	30 (compression strength)	0.85–1.00 softening coefficient
6	Zhou et al. (2021)	RM, lime, gypsum	50–60	Calcined BRM at 800 °C for 1 h, cooled down; Heated raw materials and water to 50 °C and mixed; Tested the hydration heat of the mixtures at 50 °C for 72 h				Accelerated hydration

transitioned to a harder and denser condition due to a slow self-hydration. To accelerate the cementing brick hydration and hardening process, high humidity (95%), elevated temperature (nearly 100 °C), and pressure (1–5 atm) are usually required for sample curing (1 atm=101.325 kPa) (Mymrin et al., 2003; Liu et al., 2009a; Xu et al., 2019). The cementitious activity of BRM has been proven to be activated by calcination. Zhou et al. (2021) activated BRM (bauxite tailing) by calcining it at 800 °C for 1 h. They found that in the activated BRM-lime-gypsum ternary system, BRM shortened the ending time of the induction and acceleration periods, as well as the time of occurrence of the main reaction. Moreover, the values of the main exothermic peak and the cumulative hydration heat were increased for the activated BRM.

However, due to the presence of soluble salts, such as $Mg(OH)_2$, $Ca_3Al_2(SiO_4)_3$, and $KAlSiO_4$ in BRM (Wang, 2010), the cementing brick may have efflorescence issues. Fang (2010) presented the efflorescence areas of cementing brick with 20%–80% BRM. Efflorescence on the surfaces became more

Table 5 Summary of BRM in geopolymer bricks

| No. | Reference | Raw material and mix proportion | | | Brick forming process (including pretreatment) | Characteristic | | | |
		Aluminosilicate solid	Alkaline liquid	Mix ratio		Density (g/cm^3)	Water absorption (%)	Strength (MPa)	Other
1	Mymrin and Vázquez-Vaamonde (2001)	RM, dump ferrous slags	Alkaline liquor		Mixed RM, dump ferrous slags, and alkaline liquor; Punched mixtures under 10 MPa during 1 min; Cured samples in a 98% humidity chamber			9.82	
2	Dimas et al. (2009)	RM, MK	Sodium silicate solution (8% Na$_2$O, 27% SiO$_2$, 65% H$_2$O) (in weight)	2.0–3.1 g/mL (solid to liquid ratio)	Mixed RM and MK with activator solution; Molded mixtures in 50 mm× 50 mm×50 mm molds, closed by a plastic cap at 60 °C for 6 h; Demolded and cured samples at 60 °C, 70% relative humidity for 66 h; Left samples at ambient temperature for 4 d	2.180	1.28	20.5 (compressive strength)	2.3% shrinkage
3	Kumar and Kumar (2013)	10%–20% RM, fly ash	NaOH solution (6 mol/L)	0.35 (liquid to powder ratio), 1.54–2.14 (SiO$_2$/Al$_2$O$_3$ ratio)	Mixed dry powders of RM and fly ash for 2 min followed by mixing with alkali solution for another 3 min; Casted mixtures in a plastic mold for 2 min; Cured samples at 27 °C for different periods		6	20 (on 3 d), 28 (on 28 d)	210 min initial and 300 min final setting time
4	Panias et al. (2014)	0–85% RM, MK, ferronickel slag (FeNiSG)	Sodium silicate solution (8% Na$_2$O, 27% SiO$_2$, 65% H$_2$O) (in weight)		Mixed RM, MK, and FeNiSG with the activating phase; Molded mixtures by a plastic cap at 60 °C for 6 h; Left at the ambient temperature for 18 h to be cooled; Cured samples at different temperatures (40–80 °C) and relative humidity 70% for several time periods	2.166	0.88	20±2 (compressive strength)	2.0%–3.0% shrinkage

To be continued

Table 5 (continued)

| No. | Reference | Raw material and mix proportion | | | Brick forming process (including pretreatment) | Characteristic | | | |
		Aluminosilicate solid	Alkaline liquid	Mix ratio		Density (g/cm³)	Water absorption (%)	Strength (MPa)	Other
5	Komnitsas and Zaharaki (2015)	10%–50% RM, construction demolition wastes (CDW)	NaOH solution (6, 8, and 10 mol/L); Na_2SiO_3 solution (7.5%–8.5% Na_2O, 25.5%–28.5% SiO_2) (in weight)	2.01–10.51 (SiO_2/Al_2O_3 ratio)	Mixed fly ash, electric arc furnace slag, RM, and construction/demolition wastes with alkaline solution; Cast mixtures in cubic metal mold with an edge of 5 cm; Heated at 80 or 90 °C for 7 d			51.0 (compressive strength)	
6	Kumar (2015)	20% and 40% RM, fly ash	Alkaline activator (Na_2SiO_3 to NaOH ratio is 1:1 in weight)		Mixed dry RM and fly ash for 3 min; Added alkali solution and mixed for another 3 min, added river sand and mixed for another 2 min; Molded mixtures; Cured samples at ambient temperature in closed conditions to retain the moisture		7	30 (compressive strength)	
7	Choo et al., (2016)	Five different fly ashes	0%–60% RM, 3%–10% NaOH		Mixed fly ash and RM (or fly ash and NaOH); Added water and mixed for 15 min; Poured into 50 mm cubic molds for 1 d; Placed at 60 °C for 3 d; Cured in a closed plastic container			1–4 (compressive strength)	

Table 5 (continued)

No.	Reference	Raw material and mix proportion			Brick forming process (including pretreatment)	Characteristic			
		Aluminosilicate solid	Alkaline liquid	Mix ratio		Density (g/cm^3)	Water absorption (%)	Strength (MPa)	Other
8	Kim et al. (2017)	10%–30% RM, CNF powder (Ca(OH)$_2$/NaOH/fly ash ratio= 4.3:1.0:14.7)	NaOH solution (1%, 3%, and 5% in weight)		Mixed RM slurry and deionized water; Added CNF powder and NaOH; Casted mixtures in 5 cm× 5 cm×5 cm cubic molds; Cured samples at 60 °C and 99% relative humidity for 3, 7, and 28 d			17–34 (compressive strength)	
9	Li et al. (2019)	70% RM, municipal solid waste incineration fly ash (MSWIFA)	Alkaline activator (Na$_2$SiO$_3$ to NaOH ratio is 10:1.1 in weight)	0.14 (Na$_2$SiO$_3$/ binder ratio)	Mixed RM and MSWIFA, and milled for 30 min; Added water and activator and mixed for 3 min; Pressed mixtures in a cubic mold of 20 mm; Standard curing			12.75 (compressive strength)	
10	Singh et al. (2020)	30% RM, fly ash, granulated blast furnace slag (GBFS)	Alkaline solution mixing for 10 mol/L and Na$_2$SiO$_3$/NaOH ratio as 2.5		Mixed dry raw materials; Added alkaline solution and mixed; Poured into 230 mm× 100 mm×70 mm molds; Cured at 40 °C for 4 h, and at 60 °C for 24 h	1.924– 1.998	1.14–2.35	8.7–11.1 (compressive strength)	
11	Aygörmez (2021)	Metazeolite	25% RM; sodium silicate (SiO$_2$/Na$_2$O ratio=3.29); sodium hydroxide (12 mol/L)	1.5 (binder/Na$_2$SiO$_3$ ratio), 3 (binder/ NaOH ratio)	Mixed the activator solution and binder for 2 min; Added aggregate and mixed for 3 min; Poured into molds at 50% relative humidity and 23 °C temperature for 24 h; Taken out of the molds, placed at 60 °C for 2 d; Cured in plastic storage boxes			65 (compressive strength), 11 (flexural strength)	Strength stability after the durability tests

obvious with increasing BRM content. This is due to the ionic compound (Na^+) in the alkaline BRM, which is easy to ionize, but difficult to solidify. In particular, in a humid environment (e. g., within the cementing brick), it will dissolve in water and penetrate outward, resulting in the formation of sodium salt on the brick surface. Fang (2010) found that the sodium salt content was increased by 4% in BRM cementing brick. Therefore, more attention should be paid to the durability of RM brick, especially for BRM cementing bricks. The methods and mechanisms for reducing the efflorescence will be discussed in detail in Section 5.

3.3 Production of geopolymer brick

High energy consumption and greenhouse gas emissions are the major drawbacks of firing and cementing methods to produce brick (Zhang, 2013). As an attractive alternative material, geopolymer (alkali activated material) relies on the chemical reaction of solids rich in aluminosilicate and a highly alkaline solution to form semi-crystalline aluminosilicate inorganic polymers or geopolymers (Shi et al., 2006; Duxson et al., 2007; Majidi, 2009; He et al., 2012). Since BRM is abundant in silica and alumina oxides and has a high alkaline content, it can act as a raw material (precursor or activator) in geopolymer brick. Normally, BRM geopolymer brick is manufactured using 20%–80% BRM with alkaline activators and a small amount of other aluminosilicate materials, like fly ash, metakaolin (MK), slag, and rice husk ash (RHA), depending on the chemical composition, to achieve effective geopolymerization. Table 5 summarizes the studies that used BRM in geopolymer brick.

As an alkaline activator in geopolymer brick, BRM can accelerate the dissolution of the aluminosilicate precursor, thereby increasing the polymerization rate. Choo et al. (2016) produced geopolymer (using fly ash as precursor) using BRM (high alkalinity: pH around 11) as an NaOH supplier. The 60% BRM geopolymer product had a compressive strength of 1.7 MPa, comparable to that of the control samples without BRM. Aygörmez (2021) found that a 25% BRM geopolymer brick (using metazeolite as precursor) had good performance (compressive strength of above 65 MPa, flexural strength of 11 MPa, and strength stability after the durability tests), and showed about a 12% increase in compressive strength compared

with control samples without BRM. In essence, the geopolymerization reaction is the chemical reaction of pozzolanic phases, while the oxides (CaO, SiO_2, and Al_2O_3) in raw materials play a role in the formation of hydration products and strength development in geopolymer bricks (Mendes et al., 2021).

Attempts have been made to mix BRM with a wide variety of wastes, such as fly ash, RHA, municipal solid waste incineration fly ash (MSWIFA), waste ferrous slags, and bottom ash, as the precursor in the production of geopolymers. Different oxides present in these wastes can react with the silica and alumina oxides as well as the alkaline fraction in BRM. The reaction product is usually an amorphous to semi-crystalline polymeric structure, binding the individual particles of BRM and thereby transforming the initial granular material into a compact matrix (Dimas et al., 2009). Kumar and Kumar (2013) and Kumar (2015) used BRM and fly ash to make geopolymer bricks with a strength of 30 MPa. Komnitsas and Zaharaki (2015) and Singh et al. (2020) added granulated blast furnace slag (GBFS) and electric arc furnace (EAF) slag to produce geopolymer bricks (30% BRM) with a strength of more than 50 MPa. However, some researchers found that the brick had poor flexural strength and freeze-thaw resistance, which was attributed to the 2D layered internal structure of the synthesized inorganic polymers. The layers were weakly cross-linked, probably due to an insufficient amount of aluminum in the polymeric phase (Dimas et al., 2009). To address this issue, Panias et al. (2014) added ferronickel slag and MK, which provided sufficient Al in the BRM geopolymer bricks to strengthen the bonding of the layered structure, resulting in a substantial improvement in the flexural strength and durability of the brick under moderate weathering conditions.

4 Producing brick from sintering red mud

Compared with BRM, SRM has lower alkaline leaching due to the abundance of insoluble $CaCO_3$ (Wang, 2010). Bricks made by SRM are normally immune to efflorescence and thereby have better durability. Therefore, SRM bricks are safer for applications in construction industries. Studies of the application of SRM in producing fired, cementing, and geopolymer bricks are summarized in Tables 6–8.

4.1 Production of fired brick

Table 6 lists published studies regarding the use of SRM in fired bricks. Wu et al. (2010) produced simple ceramic bricks (a kind of wall insulation material) by a normal firing method using SRM, fly ash, and clay shale as the main raw materials. The bricks exhibited good performance: 45.64% water absorption, 58.91% porosity, 1.29-g/cm^3 bulk density, 54.91-MPa compressive strength, 29.52-MPa bending strength, as well as obtaining 29.28-MPa compressive strength after freeze-thaw cycles. Lv et al. (2013) prepared fired bricks using a combination of SRM (10%−70%), shale, and sintering activation materials. The results showed that when the ratio of SRM:shale:industrial wastes was 50:35:15, the sintered bricks could meet the requirements of grade-A brick according to the GB 5101-2003 standard (GAQSIQ, 2003), and yielded 25-MPa compressive strength, 3.71-MPa flexural strength, 1.34-g/cm^3

density, and 17.57% water absorption. Gehlenite (Ca$_2$Al$_2$SiO$_7$), wollastonite (CaO·SiO$_2$), nepheline (NaAlSiO$_4$), glass phase, and remained quartz were present in the SRM fired bricks, contributing to the denser structure and higher strength of the finished brick. Ma et al. (2014) prepared a lightweight insulation brick using SRM, fly ash, and bentonite as the main raw materials along with foaming and fluxing agents. The results showed that the brick had low density (<0.67 g/cm^3) and water absorption (<5%). It was also fairly stable in preserving heat over time, implying that it had good heat insulation.

4.2 Production of cementing brick

Table 7 summarizes previous studies on the use of SRM in cementing bricks. SRM contains abundant amorphous silicon aluminates, has fine granularity and high plasticity (Feng et al., 2015), and therefore has potential cementitious activity and

Table 6 Summary of studies of SRM in fired brick

No.	Reference	Raw material	Ratio of RM (%)	Brick forming process (including pretreatment)	Characteristic			
					Density (g/cm^3)	Porosity/water absorption (%)	Strength (MPa)	Other
1	Wu et al. (2010)	RM, fly ash, clay shale	60–75	Milled raw materials; Mixed them equably, pelleted, and aged; Pressed mixtures; Fired samples at different temperatures	1.29	45.64, 58.91	54.91 (compressive strength)	5.89×10^{-3} cm^2/s thermal diffusivity and 1.15×10^{-2} W/(cm·K) conductivity
2	Lv et al. (2013)	RM, shale, sintering activated material	50	Mixed RM, shale, sintering activated material with water and displayed for 1 d; Molded mixtures at 1 MPa and 10%–14% moisture content; Dried samples for 1 h at 105 ℃; Sintered samples for 1 h at 950 ℃	1.34	17.57 (water absorption)	25.6 (compressive strength)	
3	Ma et al. (2014)	RM, fly ash, bentonite, pore forming agent, fluxing agent	7.60	Milled RM, fly ash, and bentonite; Mixed them with pore forming agent, fluxing agent, and water; Mold slurry into 40 mm× 40 mm×160 mm; Dried samples into the oven at 105 ℃ for 2 h; Fired samples at 450 ℃ slowly and keeping for 15 min, and then rising to 1100 ℃	0.6673	14 (water absorption)	2.65	

Table 7 Summary of studies of SRM in cementing bricks

No.	Reference	Raw material	Ratio of RM (%)	Brick forming process (including pretreatment)	Characteristic			
					Density (g/cm^3)	Water absorption (%)	Strength (MPa)	Other
1	Yang and Xiao (2008)	RM, fly ash, lime, gypsum, Portland cement	25–40	Mixed red mud, fly ash, sand, water, lime, and gypsum; Added Portland cement and mixed; Pressed mixtures at 20 MPa; Cured samples at room condition	1.62	22.39	29.5 (compressive strength)	0.63% shrinkage
2	Ma and Li (2013, 2014)	RM, fly ash, cement, activator, foaming agent	63	Ground RM, fly ash, and cement through 160-mesh square hole sieve; Mixed raw materials; Added activator, water, and a foaming agent; Stirred mixtures homogeneously; Poured slurry into 40 mm×40 mm× 160 mm mold; Maintained samples in the natural conditions	0.423		0.49 (flexural strength), 1.87 (compressive strength)	
3	Feng et al. (2015)	RM, fly ash, lime, gypsum, aggregate cement	30–60	Pretreated RM, fly ash, lime, and gypsum; Mixed them with aggregate and cement; Added water and mixed; Formed mixtures at 15 MPa; Maintained samples at room condition		14–18	18.32 (compressive strength), 3.53 (flexural strength)	
4	Zhao et al. (2020)	RM, cement, fly ash, lime	25, 30, 35	Mixed RM, cement, fly ash, and lime; Added water and mixed; Poured, vibrated mixtures; Pressed them in mold; Cured samples	1.87	15.8	19.14 (compressive strength), 15.4 (after 25 freeze-thaw cycles)	0.04% shrinkage
5	Zhao and Gou (2021)	RM, calcium sulfoaluminate (CSA) cement	30–70	Mixed RM and CSA cement; Added water and mixed; Poured, vibrated mixtures; Pressed them in mold; Cured samples	2.45 (dry density)	8–10	30–60 (compressive strength)	Low metal leaching

excellent properties for cementing brick preparation. Zhao and Gou (2021) prepared cementing bricks by incorporating SRM in calcium sulfoaluminate cement (binary blends), and found that the 70% SRM bricks had a compressive strength of 30–35 MPa. The soluble Na in SRM promoted the hydration of C_4A_3 and C_2S. SRM also reduced the porosity of the hydration products of the binary blends. On the other hand, the soluble Na and F could be immobilized by the precipitation of AlF_3 and CaF_2, respectively. Note that the dissolution of heavy metals was prevented, which satisfies the requirements detailed in GB 5749-2006 (NHC, 2006) and GB 6566-2010 (GAQSIQ, 2010; Zhao and Gou, 2021).

A cement-fly ash-lime system was proven to be effective in stabilizing SRM. SRM cementing bricks were prepared with 20%–70% SRM, 18%–30% fly ash, 6%–10% lime, and 1%–15% cement. The C-S-H gel and ettringite present in the bricks were responsible for the improved performance. Feng et al. (2015) produced the cementing bricks by mixing 44%–55% SRM, 19%–30% fly ash, 6%–7% lime, 4%–6% α-hemihydrate gypsum, 25%–35% Yellow River silt, and 2% ordinary cement, with a water to binder ratio of 14%–18%. Then, the mixtures were molded under 15-MPa pressure and cured at room temperature for 12 h. The 28-d compressive strength of the produced brick was up to 18 MPa, meeting the standard requirements of bricks. Yang and Xiao (2008) proposed that the optimal proportions of the materials in SRM bricks were 25%–40% SRM, 18%–28% fly ash, 30%–35% sand, 8%–10% lime, 1%–3% gypsum, and about 1% Portland cement. The produced SRM cementing brick could achieve 29.5-MPa compressive strength, 22.39% water absorption, 1.62-g/cm³ density, and 0.63% shrinkage. However, Zhao et al. (2020) reported that the optimal proportions of SRM brick constituents were 35% RM, 14% fly ash, 8% lime, 15% cement, and 28% sand. These bricks had the best performance with a compressive strength of more than 19 MPa after 25 freeze-thaw cycles, water absorption of 15.8%, and shrinkage of 0.04%.

Ma and Li (2013, 2014) studied the effect of activator and foaming agents on the properties of lightweight cementing bricks prepared with SRM. The results showed that by mixing 1% activator and 10-mL foaming agent per 390-g mix, the bricks attained low density (423 kg/m³) and gained a 64.4% and 44.1% increase in the flexural strength (0.49 MPa) and compressive strength (1.87 MPa), respectively, compared to samples without additives. The improvement in properties was attributed to the additives inducing an even distribution of closed pores in the SRM cementing bricks.

Overall, previous studies showed that it is feasible to use SRM to produce cementing bricks, due to its higher CaO content and abundant C_2S phase, which give rise to its cementitious activity (Yang et al., 2006; Sutar et al., 2014). The properties of the SRM cementing bricks are influenced by the formation and microstructure of C-S-H, ettringite, and hydration products.

4.3 Production of geopolymer brick

Table 8 lists studies on the use of SRM in geopolymer bricks. Zhang et al. (2011) investigated the pozzolanic behavior of the compound-activated SRM-coal gangue-lime system and pointed out that the hydration products were mainly aluminous C-S-H, $Ca_3Al_2O_6 \cdot xH_2O$, and a high content of $Ca(OH)_2$. Thus, it is feasible to use SRM as a raw material in producing geopolymer bricks. Fu and Xiong (2014) mixed 30% gypsum, 10% RM and fly ash, and 20% lime to prepare an SRM-based geopolymer with a compressive strength of 15.44 MPa. Zhou et al. (2020) used 30%–70% refuse mudstone, GBFS, and SRM as the precursor materials, and water glass as the alkaline activator, to produce geopolymer composites containing 21% SRM. The end products had the highest unconfined compressive strength of 23.48 MPa and the highest Brazil tensile strength of 2.98 MPa. Scanning electron microscopy (SEM) observations revealed that the SRM geopolymer composites had a compact microstructure. However, larger-scale studies are needed to explore the mix proportion, manufacturing methods, performance, and mechanisms of SRM geopolymer bricks.

5 Discussion

5.1 Comparison between BRM and SRM in RM-modified brick

The advantages and disadvantages of different types of RM-modified bricks are reviewed and summarized in Table 9. Regardless of the brick type, 20%–80% RM can be used to produce bricks. Different

Table 8 Summary of studies of SRM in geopolymer materials

No.	Reference	Raw material	Ratio of RM (%)	Sample preparation process (including pretreatment)	Strength (MPa)
1	Zhang et al. (2011)	RM, coal gangue, lime	60	Mixed RM, coal gangue, water, and pelleted; Dried at 100 °C for 6 h, fired at 600 °C for 2 h; Milled for 6 min; Obtained compound-activated RM-coal gangue (pretreatment); Mixed compound-activated RM-coal gangue (80%–90%) and CaO (10%–20%) (in weight); Cured samples in a humidity chamber at 20 °C and constant 95% relative humidity	
2	Fu and Xiong (2014)	RM, fly ash, lime	30	Mixed raw materials; Added water and mixed for 3 min; Put the slurry in molds and put the molds into a wet box at 20 °C for 24 h; Demold and cured samples into the box again for 28 d	15.43 (compressive strength)
3	Zhou et al. (2020)	RM, GBFS, mudstone, sand, NaOH, water glass	9–21	Crushed, grounded, and seized red mud; Mixed dry raw materials; Added alkaline activator and mixed for 3 min; Added standard sand and mixed for another 3 min; Cast mixtures into plastic molds and vibration for 1 min; Cured samples for 28 d at 20 °C and >90% humidity	23.48 (unconfined compressive strength), 2.98 (Brazil tensile strength)

Table 9 Comparison of bricks made with different RMs

Type of brick	Ratio of RM (%)	Additive or activator	Innovative way of making brick	Advantage	Disadvantage
Fired brick	20–80 (BRM)	Clay, fly ash, etc.	Ground and preheated raw BRM at 100 °C; Digested RM with 2 mol/L NaOH at 135–150 °C; Dried samples before calcination; Frozen and thawed samples before calcination; Modified BRM by dewatering; Pressed samples in three equal layers	High strength (up to 54 MPa)	High energy consumption, high CO_2 emission
	50–80 (SRM)		Adding sintering activated material; Dried samples before calcination; Modified BRM by dewatering		
Cementing brick	70–100 (BRM)	Cement, lime, fly ash, gypsum, etc.	Recovering iron from BRM before making bricks; Adding activator; Pretreating raw materials: drying, grinding, etc.	Low energy consumption, low CO_2 emission	Normal strength (about 10–30 MPa) and durability (efflorescence)
	20–60 (SRM)		Adding activator; Pretreating raw materials: drying, grinding, etc.		
Geopolymer brick	20–80 (BRM) 30–100 (SRM)	Coal gangue, fly ash, MK, slag, RHA, etc.	Cured samples at above room temperature (40–100 °C) and high humidity Making compound-activated RM-coal gangue material as the precursor by adding alkaline and firing at 100–600 °C; Accelerate carbonation	High strength (up to 51 MPa), good durability, lower energy consumption, lower CO_2 emission	

materials were used as the additive/activator/precursor for RM bricks to stimulate the RM activity. For example, clay and fly ash were added for RM fired bricks, and cement, lime, fly ash, and gypsum were mixed for RM cementing bricks. Coal gangue, fly ash, MK, slag, and RHA were used as the precursors for RM geopolymer bricks. To produce a more environmentally-friendly brick, metal minerals can first be recovered from RM. Alternatively, innovative technology, such as accelerated carbonation, can be used to improve the RM reactivity.

Fired bricks have been the most used product because of their high strength (up to 54 MPa) (Nivetha et al., 2017). From an environmental protection perspective, however, they are undesirable due to their high energy consumption and CO_2 emissions during the firing process. Instead, RM cementing bricks are more environmental-friendly, although they have a lower performance in terms of their mechanical properties (e.g., lower compressive strength) and durability (e.g., higher water absorption and potential efflorescence) (Wang et al., 2011; Yin et al., 2011). RM geopolymer bricks seem to represent a promising new approach to overcome some of the above-mentioned drawbacks, with high strength (up to 51 MPa), good durability (no efflorescence), and lower energy consumption and CO_2 emissions (Singh et al., 2016).

The RMs produced from different processes (Bayer and sintering) have different salient features for each type of brick. BRM is usually used to produce fired and geopolymer bricks since it contains a higher amount of Al_2O_3, SiO_2, and alkaline phases (higher pH), which are more favorable for calcination and geopolymerization. On the other hand, SRM is more suitable for cementing brick manufacture due to its higher CaO content and abundant C_2S phase, which give rise to better cementitious activity.
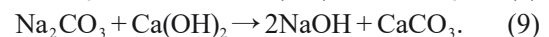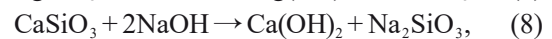
In addition to the three types of bricks discussed, an innovative brick has been developed by simply mixing RM with water cured by accelerated carbonation at room temperature (Liu et al., 2017b). This SRM-based ceramic brick was prepared as follows: SRM and water were mixed for 10 min at a constant ratio of 1:10, followed by extrusion into a mold with 20-MPa extruding pressure. The semi-finished brick was then immediately placed into a sealed carbonation chamber with 99.9% CO_2, at 0.3-MPa CO_2 pressure, 98% relative humidity, and (23±2) °C. The brick

was carbonated for 5 and 24 h to obtain 23.1- and 25.0-MPa compressive strengths, respectively. In addition, up to 100 kg of CO_2 was sequestrated per ton of SRM used. The strength enhancement was attributed to the formation of crystalline calcium carbonate and amorphous silica gels during the carbonation process. Therefore, as a raw material for manufacturing bricks, RM can be used not only with other solid wastes, but also with agricultural and industrial wastes, such as gas waste and liquid waste, in an attempt to maximize environmental protection in a cost-effective way.

5.2 Efflorescence consideration

The main reason that RM has not been widely used to produce bricks is the potential efflorescence issue (Fang, 2010). Besides negatively affecting the brick's appearance, it also deteriorates the bonding between the brick and mortar. As a result, the brick strength and durability are impaired, leading to serious damage to the masonry structure. Therefore, it is necessary to understand the efflorescence mechanism and find a viable method to solve this vexing problem.

In a humid environment, sodium alkali or salt (e.g., NaOH or Na_2CO_3) in RM will easily dissolve and ionize to produce OH^-, which reacts with oxides such as CaO or MgO. Afterwards, it penetrates outwards and migrates to the brick surface, forming efflorescence (Chen, 2016). The main reactions are described as follows (Fang, 2010):

$$MgSiO_3 + 2NaOH \rightarrow Mg(OH)_2 + Na_2SiO_3, \quad (7)$$
$$CaSiO_3 + 2NaOH \rightarrow Ca(OH)_2 + Na_2SiO_3, \quad (8)$$
$$Na_2CO_3 + Ca(OH)_2 \rightarrow 2NaOH + CaCO_3. \quad (9)$$

Compared with insoluble salts, soluble salts have a much bigger impact on the efflorescence level due to their higher alkalinity (Xing, 2010). SRM consists mainly of insoluble $CaCO_3$, followed by NaCl, KCl, $CaTiO_3$, FeN, and KF. In contrast, the main alkali constituents of BRM are soluble salts, such as $NaNO_3$, $Mg(OH)_2$, $Ca_3Al_2(SiO_4)_3$, and $KAlSiO_4$ (Wang, 2010). Thus, compared with SRM bricks, BRM bricks are prone to more severe efflorescence. Compared with fired bricks and geopolymers, BRM cementing bricks experience the greatest formation of efflorescence because almost all of the alkaline phases in BRM dissolve in water, penetrate outwards, and migrate to the brick surface. Geopolymer has a lower propensity

for efflorescence due to the use of parts of alkaline phases as an activator. The fired bricks are the least affected by efflorescence. This is because the soluble alkaline substances in BRM are converted into insoluble salts during the firing process (Xing, 2010; Rai et al., 2013).

To solve the efflorescence issue, many approaches have been used to reduce the alkalinity of cementing bricks, including double reverse washing (Wang, 2010), adding lime to dissolve the BRM at 170 °C and 0.9 MPa (Zhong et al., 2009), a suspension carbonation method (Wang et al., 2009), and a slurry multi-stage cycle method (Yang et al., 2012). However, viable approaches with satisfactory results remain elusive. Further studies are needed to ascertain the applicability of de-alkaline processes in a larger-scale industrial setting.

5.3 Radioactivity concerns

One of the major concerns of using RM in brick production is its radioactivity, requiring strict compliance with regulations (Brunori et al., 2005; Santona et al., 2006; Somlai et al., 2008; Gu et al., 2011; Luo et al., 2013). Bauxite is associated with high radionuclides and trace elements, such as uranium, thorium, radium-226, and potassium-40. These elements exist in some minerals, such as zircon and monazite, which are difficult to remove during alumina production (Luo et al., 2013). Usually, these radioactive elements can penetrate several meters thickness of cement concrete, producing ionizing radiation that can greatly harm human health (Gu et al., 2011). Unlike stabilizing or solidifying heavy metals, radioactivity cannot be contained easily in solid materials (Hegedűs et al., 2016).

Two main types of methods have been proposed to reduce the risks from radioactivity: reducing the self-radioactivity of RM and adopting radioactive shielding measures. Qin and Wu (2011) found that the radioactivity levels of RM (6360 Bq) could be reduced to the natural radioactive background level in Guilin, China (3600 Bq) when producing self-glazing RM-based ceramic materials, owing to the sintering process. This also can be achieved by removing the radioactive minerals from RM using magnetic separation. For radioactive shielding, spraying surfactant such as anti-radiation functional mortar or paint has also been proven to be effective (Luo et al., 2013). Tian et al. (2015) and Wang et al. (2016) suggested that using

barite, which contains barium (Ba) atomic energy and boron elements, could activate the attenuation of radiation energy, particularly for X-ray absorption (Mann et al., 2013; Wang et al., 2016). Boron-rich slag can also offer effective radiation shielding (Tian et al., 2016). However, to ascertain safeness for construction and building applications, tests of the internal exposure index (I_{Ra}) and external exposure index (I_r) should be carried out. In China, RM bricks must be tested and meet the Chinese standard GB 6566-2010 (GAQSIQ, 2010) before they can be introduced into the construction industry (Zhang et al., 2018, 2021).

6 Conclusions

In this paper, the characteristics of BRM and SRM were compared and their applications in the production of different bricks including fired, cementing, and geopolymer bricks were thoroughly reviewed. Several conclusions can be drawn:

BRM with high alkalinity is generated from caustic soda in the alumina production process and has a high Al_2O_3 content derived from the bauxite resource, whereas SRM has lower alkalinity with a certain cementitious property because of the amorphous aluminosilicate generated from the high temperature sintering process. The addition of limestone in the sintering process results in the presence of a high CaO content in SRM. As a result, efflorescence is the main issue for BRM cementing bricks due to high alkalinity and content of free oxides, as explained in Section 5. To date, there is no effective way to solve this problem. Compared with BRM cementing bricks, BRM fired bricks and geopolymer bricks are more durable and stronger. Therefore, BRM is considered as a good raw material to produce these two types of bricks.

SRM has received less research attention than BRM due to the complexity of the sintering process. Only a few studies have investigated the feasibility of using SRM in bricks. However, SRM is not suitable for manufacturing fired bricks because an intensive manufacturing process is required to solidify and stabilize the alkalinity. Instead, SRM is considered as a better option in the production of cementing bricks due to the presence of abundant amorphous aluminosilicate. Compared with fired and cementing bricks, geopolymer bricks usually have better strength and

durability because of the high alkalinity of RM, which is favorable for the geopolymerization reaction.

There is an urgent need to address the efflorescence issue in RM-modified bricks, especially BRM cementing bricks, because efflorescence is the key issue that greatly limits the wide use of RM in brick production. Regarding the potential radiation issue, several solutions have been suggested in the literature, though it is not considered a great concern as long as the use of RM meets the standard regulations. Therefore, recycling and reusing RM in the production of bricks are still recommended to reduce environmental contamination and enhance the brick properties. Process optimization of RM brick production, especially geopolymer bricks, should be systematically investigated to broaden its application. More importantly, innovative and economically viable methods, such as carbonation of RM, should be given attention to develop new types of environmentally-friendly RM bricks at an industry scale. Last, but not least, to have larger-scale RM applications in the future, it is necessary to analyze the economic benefits and costs of RM bricks.

Author contributions

Yu-jia XIAO wrote the first draft of the manuscript. Michelle TIONG, Kim Hung MO, Ming-zhi GUO, and Tung-chai LING helped to organize the manuscript. Tung-chai LING, Michelle TIONG, and Yu-jia XIAO revised and edited the final version.

Conflict of interest

Yu-jia XIAO, Michelle TIONG, Kim Hung MO, Ming-zhi GUO, and Tung-chai LING declare that they have no conflict of interest.

References

Alekseev K, Mymrin V, Avanci MA, et al., 2019. Environmentally clean construction materials from hazardous bauxite waste red mud and spent foundry sand. *Construction and Building Materials*, 229:116860. https://doi.org/10.1016/j.conbuildmat.2019.116860

Annan E, Agyei-Tuffour B, Damoah LNW, et al., 2012. Physico-mechanical properties of bauxite residue-clay bricks. *Journal of Engineering and Applied Sciences*, 7(12):1587-1594.

Arroyo F, Luna-Galiano Y, Leiva C, et al., 2020. Environmental risks and mechanical evaluation of recycling red mud in bricks. *Environmental Research*, 186:109537. https://doi.org/10.1016/j.envres.2020.109537

Aygörmez Y, 2021. Evaluation of the red mud and quartz sand on reinforced metazeolite-based geopolymer composites. *Journal of Building Engineering*, 43:102528. https://doi.org/10.1016/j.jobe.2021.102528

Babisk MP, Amaral LF, da Silva Ribeiro L, et al., 2020. Evaluation and application of sintered red mud and its incorporated clay ceramics as materials for building construction. *Journal of Materials Research and Technology*, 9(2):2186-2195. https://doi.org/10.1016/j.jmrt.2019.12.049

Bi SW, 2006. Alumina Refining Technology. Chemical Industry Press, Beijing, China (in Chinese).

Brunori C, Cremisini C, Massanisso P, et al., 2005. Reuse of a treated red mud bauxite waste: studies on environmental compatibility. *Journal of Hazardous Materials*, 117(1):55-63. https://doi.org/10.1016/j.jhazmat.2004.09.010

Chen C, 2016. Mechanism and treatment measures of frost flooding in autoclaved aerated concrete block. *Wall Materials Innovation & Energy Saving in Building*, (10):30-33 (in Chinese).

Choo H, Lim S, Lee W, et al., 2016. Compressive strength of one-part alkali activated fly ash using red mud as alkali supplier. *Construction and Building Materials*, 125:21-28. https://doi.org/10.1016/j.conbuildmat.2016.08.015

Dimas DD, Giannopoulou IP, Panias D, 2009. Utilization of alumina red mud for synthesis of inorganic polymeric materials. *Mineral Processing and Extractive Metallurgy Review*, 30(3):211-239. https://doi.org/10.1080/08827500802498199

Duxson P, Fernández-Jiménez A, Provis JL, et al., 2007. Geopolymer technology: the current state of the art. *Journal of Materials Science*, 42(9):2917-2933. https://doi.org/10.1007/s10853-006-0637-z

Fang YG, 2010. Study on High Alkaline Red Mud as Resources and Its Application. PhD Thesis, Wuhan University of Technology, Wuhan, China (in Chinese).

Feng YL, Yu LJ, Gao JP, et al., 2015. Study on the preparation and properties of red mud unburned brick. *Materials Research Innovations*, 19(S8):S8-297-S8-300. https://doi.org/10.1179/1432891715Z.0000000001686

Fu Y, Xiong ZQ, 2014. Red mud based geopolymer and its forming mechanism. *Applied Mechanics and Materials*, 538:28-31. https://doi.org/10.4028/www.scientific.net/AMM.538.28

GAQSIQ (General Administration of Quality Supervision, Inspection and Quarantine of the People's Republic of China), 2003. Fired Common Bricks, GB 5101-2003. GAQSIQ, Beijing, China (in Chinese).

GAQSIQ (General Administration of Quality Supervision, Inspection and Quarantine of the People's Republic of China), 2010. Limits of Radionuclides in Building Materials, GB 6566-2010. GAQSIQ, Beijing, China (in Chinese).

Gu HN, Wang N, Zhang NC, et al., 2011. Study on radioactivity level of red mud and radiological constraints of usability

as building materials. *Light Metals*, (5):19-21 (in Chinese).
https://doi.org/10.13662/j.cnki.qjs.2011.05.017

Han YF, Yang JJ, Wang X, et al., 2011. Research on the basic characteristics and utilization value of the sintering process and Bayer process red mud. *Materials Review*, 25(11):122-125 (in Chinese).
https://doi.org/10.1016/j.jhazmat.2011.11.095

He J, Zhang JH, Yu YZ, et al., 2012. The strength and microstructure of two geopolymers derived from metakaolin and red mud-fly ash admixture: a comparative study. *Construction and Building Materials*, 30:80-91.
https://doi.org/10.1016/j.conbuildmat.2011.12.011

Hegedűs M, Sas Z, Tóth-Bodrogi E, et al., 2016. Radiological characterization of clay mixed red mud in particular as regards its leaching features. *Journal of Environmental Radioactivity*, 162-163:1-7.
https://doi.org/10.1016/j.jenvrad.2016.05.002

Kalkan E, 2006. Utilization of red mud as a stabilization material for the preparation of clay liners. *Engineering Geology*, 87(3-4):220-229.
https://doi.org/10.1016/j.enggeo.2006.07.002

Kavas T, 2006. Use of boron waste as a fluxing agent in production of red mud brick. *Building and Environment*, 41(12):1779-1783.
https://doi.org/10.1016/j.buildenv.2005.07.019

Kelessidis VC, Tsamantaki C, Dalamarinis P, 2007. Effect of pH and electrolyte on the rheology of aqueous Wyoming bentonite dispersions. *Applied Clay Science*, 38(1-2):86-96.
https://doi.org/10.1016/j.clay.2007.01.011

Khairul MA, Zanganeh J, Moghtaderi B, 2019. The composition, recycling and utilisation of Bayer red mud. *Resources, Conservation and Recycling*, 141:483-498.
https://doi.org/10.1016/j.resconrec.2018.11.006

Kim SY, Jun Y, Jeon D, et al., 2017. Synthesis of structural binder for red brick production based on red mud and fly ash activated using Ca(OH)$_2$ and Na$_2$CO$_3$. *Construction and Building Materials*, 147:101-116.
https://doi.org/10.1016/j.conbuildmat.2017.04.171

Kim Y, Lee Y, Kim M, et al., 2019. Preparation of high porosity bricks by utilizing red mud and mine tailing. *Journal of Cleaner Production*, 207:490-497.
https://doi.org/10.1016/j.jclepro.2018.10.044

Klauber C, Gräfe M, Power G, 2011. Bauxite residue issues: II. Options for residue utilization. *Hydrometallurgy*, 108(1-2):11-32.
https://doi.org/10.1016/j.hydromet.2011.02.007

Komnitsas K, Zaharaki D, 2015. Co-utilization of construction and demolition with industrial wastes for the production of geopolymers. International Conference on Industrial Waste & Wastewater Treatment & Valorization.

Kumar A, Kumar S, 2013. Development of paving blocks from synergistic use of red mud and fly ash using geopolymerization. *Construction and Building Materials*, 38:865-871.
https://doi.org/10.1016/j.conbuildmat.2012.09.013

Kumar S, 2015. The properties and performance of red mud-based geopolymeric masonry blocks. *In*: Pacheco-Torgal F, Lourenço PB, Labrincha JA, et al. (Eds.), Eco-efficient Masonry Bricks and Blocks: Design, Properties and Durability. Woodhead Publishing, Cambridge, UK, p.311-328.

Li YC, Min XB, Ke Y, et al., 2019. Preparation of red mud-based geopolymer materials from MSWI fly ash and red mud by mechanical activation. *Waste Management*, 83:202-208.
https://doi.org/10.1016/j.wasman.2018.11.019

Liu DY, Wu CS, 2012. Stockpiling and comprehensive utilization of red mud research progress. *Materials*, 5(7):1232-1246.
https://doi.org/10.3390/ma5071232

Liu SH, Guan XM, Zhang SS, et al., 2017a. Sintered Bayer red mud based ceramic bricks: microstructure evolution and alkalis immobilization mechanism. *Ceramics International*, 43(15):13004-13008.
https://doi.org/10.1016/j.ceramint.2017.07.036

Liu SH, Guan XM, Zhang SS, et al., 2017b. Sintering red mud based imitative ceramic bricks with CO$_2$ emissions below zero. *Materials Letters*, 191:222-224.
https://doi.org/10.1016/j.matlet.2016.12.028

Liu WC, Yang JK, Xiao B, 2009a. Application of Bayer red mud for iron recovery and building material production from alumosilicate residues. *Journal of Hazardous Materials*, 161(1):474-478.
https://doi.org/10.1016/j.jhazmat.2008.03.122

Liu WC, Yang JK, Xiao B, 2009b. Review on treatment and utilization of bauxite residues in China. *International Journal of Mineral Processing*, 93(3-4):220-231.
https://doi.org/10.1016/j.minpro.2009.08.005

Liu XM, Zhang N, 2013. Utilization of red mud in cement production: a review. *Waste Management & Research: the Journal for a Sustainable Circular Economy*, 29(10):1053-1063.
https://doi.org/10.1177/0734242X11407653

Luo ZT, Zhang MX, Wang X, et al., 2013. Present situation of radiation shielding technology for red mud in building material field. *Light Metals*, (9):16-18 (in Chinese).
https://doi.org/10.13662/j.cnki.qjs.2013.09.013

Lv CS, Wang JW, Zhao PY, et al., 2013. Effect of red mud content on the property of sintered brick. *Advanced Materials Research*, 726-731:2677-2680.
https://doi.org/10.4028/www.scientific.net/AMR.726-731.2677

Ma L, Li GZ, 2013. Activator on properties of red mud lightweight baking-free brick. *Applied Mechanics and Materials*, 468:36-38.
https://doi.org/10.4028/www.scientific.net/AMM.468.36

Ma L, Li GZ, 2014. Influence of foaming agent on properties of red mud lightweight baking-free brick. *Applied Mechanics and Materials*, 541-542:388-391.
https://doi.org/10.4028/www.scientific.net/AMM.541-542.388

Ma L, Li GZ, Hu JR, 2014. Heat preservation time on the properties of red mud lightweight insulation brick. *Applied Mechanics and Materials*, 540:225-228.
https://doi.org/10.4028/www.scientific.net/AMM.540.225

Majidi B, 2009. Geopolymer technology, from fundamentals to advanced applications: a review. *Materials Technology*, 24(2):79-87.

https://doi.org/10.1179/175355509X449355

Mandal AK, Sinha OP, 2017. Effect of bottom ash fineness on properties of red mud geopolymer. *The Journal of Solid Waste Technology and Management*, 43(1):26-35. https://doi.org/10.5276/JSWTM.2017.26

Mandal AK, Verma HR, Sinha OP, 2017. Utilization of aluminum plant's waste for production of insulation bricks. *Journal of Cleaner Production*, 162:949-957. https://doi.org/10.1016/j.jclepro.2017.06.080

Mann KS, Kaur B, Sidhu GS, et al., 2013. Investigations of some building materials for γ-rays shielding effectiveness. *Radiation Physics and Chemistry*, 87:16-25. https://doi.org/10.1016/j.radphyschem.2013.02.012

Mendes BC, Pedroti LG, Vieira CMF, et al., 2021. Application of eco-friendly alternative activators in alkali-activated materials: a review. *Journal of Building Engineering*, 35: 102010. https://doi.org/10.1016/j.jobe.2020.102010

Meyer FM, 2004. Availability of bauxite reserves. *Natural Resources Research*, 13(3):161-172. https://doi.org/10.1023/B:NARR.0000046918.50121.2e

Mi HC, Yi LS, Wu Q, et al., 2021. Preparation of high-strength ceramsite from red mud, fly ash, and bentonite. *Ceramics International*, 47(13):18218-18229. https://doi.org/10.1016/j.ceramint.2021.03.141

Mymrin V, de Araújo Ponte H, Lopes OF, et al., 2003. Environment-friendly method of high alkaline bauxite's red mud and ferrous slag utilization as an example of green chemistry. *Green Chemistry*, 5(3):357-360. https://doi.org/10.1039/B300495N

Mymrin VA, Vázquez-Vaamonde AJ, 2001. Red mud of aluminium production waste as basic component of new construction materials. *Waste Management & Research: the Journal for a Sustainable Circular Economy*, 19(5):465-469. https://doi.org/10.1177/0734242X0101900512

NHC (National Health Commission of the People's Republic of China), 2006. Standards for Drinking Water Quality, GB 5749-2006. NHC, Beijing, China (in Chinese).

Nivetha C, Johnson RD, Lakshminarayana V, 2017. Study on strength and behavior of red mud bricks. *Journal of Industrial Pollution Control*, 33(S2):1227-1230.

Panias D, Giannopoulou I, Boufounos D, 2014. Valorization of alumina red mud for production of geopolymeric bricks and tiles. *In*: Grandfield J (Ed.), Light Metals 2014. Springer, Cham, Switzerland, p.155-159. https://doi.org/10.1007/978-3-319-48144-9_27

Power G, Gräfe M, Klauber C, 2011. Bauxite residue issues: I. Current management, disposal and storage practices. *Hydrometallurgy*, 108(1-2):33-45. https://doi.org/10.1016/j.hydromet.2011.02.006

Qin S, Wu BL, 2011. Effect of self-glazing on reducing the radioactivity levels of red mud based ceramic materials. *Journal of Hazardous Materials*, 198:269-274. https://doi.org/10.1016/j.jhazmat.2011.10.039

Rai S, Lataye DH, Chaddha MJ, et al., 2013. An alternative to clay in building materials: red mud sintering using fly ash via Taguchi's methodology. *Advances in Materials Science and Engineering*, 2013:757923.

https://doi.org/10.1155/2013/757923

Rehman MU, Ahmad M, Rashid K, 2020. Influence of fluxing oxides from waste on the production and physico-mechanical properties of fired clay brick: a review. *Journal of Building Engineering*, 27:100965. https://doi.org/10.1016/j.jobe.2019.100965

Samal S, Ray AK, Bandopadhyay A, 2013. Proposal for resources, utilization and processes of red mud in India—a review. *International Journal of Mineral Processing*, 118: 43-55. https://doi.org/10.1016/j.minpro.2012.11.001

Santona L, Castaldi P, Melis P, 2006. Evaluation of the interaction mechanisms between red muds and heavy metals. *Journal of Hazardous Materials*, 136(2):324-329. https://doi.org/10.1016/j.jhazmat.2005.12.022

Scribot C, Maherzi W, Benzerzour M, et al., 2018. A laboratory-scale experimental investigation on the reuse of a modified red mud in ceramic materials production. *Construction and Building Materials*, 163:21-31. https://doi.org/10.1016/j.conbuildmat.2017.12.092

Sglavo VM, Campostrini R, Maurina S, et al., 2000a. Bauxite 'red mud' in the ceramic industry. Part 1: thermal behaviour. *Journal of the European Ceramic Society*, 20(3): 235-244. https://doi.org/10.1016/S0955-2219(99)00088-6

Sglavo VM, Maurina S, Conci A, et al., 2000b. Bauxite 'red mud' in the ceramic industry. Part 2: production of clay-based ceramics. *Journal of the European Ceramic Society*, 20(3):245-252. https://doi.org/10.1016/S0955-2219(99)00156-9

Shi CJ, Krivenko PV, Roy D, 2006. Alkali-activated Cements and Concretes. CRC Press, New York, USA.

Shoppert AA, Loginova IV, Rogozhnikov DA, et al., 2019. Increased as adsorption on maghemite-containing red mud prepared by the alkali fusion-leaching method. *Minerals*, 9(1):60. https://doi.org/10.3390/min9010060

Singh IB, Jawaid SMA, 2015. Analysis of the compressive strength of a brick formed from industrial waste (red mud). *International Journal for Scientific Research & Development*, 3(6):889-893.

Singh KK, Singh VK, Mankhand TR, et al., 2014. Utilization of Indian red mud and fly ash with combustible additives to prepare foam bricks. Proceedings of the International Conference on Energy, Environment, Materials and Safety, p.551-556.

Singh S, Basavanagowda SN, Aswath MU, et al., 2016. Durability of bricks coated with red mud based geopolymer paste. *IOP Conference Series: Materials Science and Engineering*, 149:012070. https://doi.org/10.1088/1757-899X/149/1/012070

Singh S, Aswath MU, Ranganath RV, 2020. Performance assessment of bricks and prisms: red mud based geopolymer composite. *Journal of Building Engineering*, 32:101462. https://doi.org/10.1016/j.jobe.2020.101462

Somlai J, Jobbágy V, Kovács J, et al., 2008. Radiological aspects of the usability of red mud as building material additive. *Journal of Hazardous Materials*, 150(3):541-545.

https://doi.org/10.1016/j.jhazmat.2007.05.004

Sun CW, Chen JN, Tian K, et al., 2019. Geochemical characteristics and toxic elements in alumina refining wastes and leachates from management facilities. *International Journal of Environmental Research and Public Health*, 16(7):1297.
https://doi.org/10.3390/ijerph16071297

Sutar H, Mishra SC, Sahoo SK, et al., 2014. Progress of red mud utilization: an overview. *American Chemical Science Journal*, 4(3):255-279.
http://doi.org/10.9734/ACSJ/2014/7258

Tian CF, Luo ZT, Wang X, et al., 2015. Influence research of barite on strength and radioactive of red mud cement mortar. *China Concrete and Cement Products*, (4):59-62 (in Chinese).
https://doi.org/10.19761/j.1000-4637.2015.04.015

Tian CF, Luo ZT, Wang X, et al., 2016. Study of impact of steel slag on the strength and radioactive of the red mud P·C mortar. *Concrete*, 2:124-127.
https://doi.org/10.3969/j.issn.1002-3550.2016.02.031

Wang LL, 2010. The Analysis of Red Mud Alkaline and the Study of Bulk Comprehensive Utilization—to Jiaozuo Aluminum Zhongzhou Bayer New Red Mud as an Example. MS Thesis, Henan Polytechnic University, Jiaozuo, China (in Chinese).

Wang Q, Li J, Zhao Y, et al., 2009. Study on the dealkalization of red mud by suspension and carbonation. *Chinese Journal of Environmental Engineering*, 3(12):2275-2280 (in Chinese).

Wang X, Tian CF, Luo ZT, et al., 2016. Effecting research of zeolite on strength and radioactive properties of red mud cement mortar. *China Concrete and Cement Products*, (1):23-26 (in Chinese).
https://doi.org/10.19761/j.1000-4637.2016.01.006

Wang XY, Yin GX, Xing MF, 2011. Composition analysis of hoarfrost of alumina plant's red mud. *Journal of Henan Polytechnic University (Natural Science)*, 30(3):361-365 (in Chinese).
https://doi.org/10.16186/j.cnki.1673-9787.2011.03.025

Wu JF, Zhang FY, Li HL, et al., 2010. Preparation and reaction mechanism of red mud based ceramic simple bricks. *Journal of Wuhan University of Technology (Materials Science Edition)*, 25(6):1001-1005.
https://doi.org/10.1007/s11595-010-0138-4

Xing MF, 2010. The Study on Floating Hoarfrost of Zhongzhou Aluminum Plant Multi-year Sintered Red Mud and the Production of Red Mud Bricks. MS Thesis, Henan Polytechnic University, Jiaozuo, China (in Chinese).

Xu YT, Yang B, Liu XM, et al., 2019. Investigation of the medium calcium based non-burnt brick made by red mud and fly ash: durability and hydration characteristics. *International Journal of Minerals, Metallurgy, and Materials*, 26(8):983-991.
https://doi.org/10.1007/s12613-019-1814-9

Yang JJ, Li JW, Xiao YL, et al., 2012. Research on dealkalization of sintering process red mud by lime process at normal atmosphere and mechanism thereof. *Inorganic Chemicals Industry*, 44(6):40-42 (in Chinese).
https://doi.org/10.3969/j.issn.1006-4990.2012.06.013

Yang JK, Xiao B, 2008. Development of unsintered construction materials from red mud wastes produced in the sintering alumina process. *Construction and Building Materials*, 22(12):2299-2307.
https://doi.org/10.1016/j.conbuildmat.2007.10.005

Yang JK, Hou J, Qi B, et al., 2006. Pilot-scale production and industrialization of the no-fired bricks from red mud in aluminium industry. *Environmental Engineering*, 24(4):52-55 (in Chinese).
https://doi.org/10.3969/j.issn.1000-8942.2006.04.018

Yang ZY, 1993. Alumina Production Technology. Metallurgical Industry Press, Beijing, China (in Chinese).

Yin GX, Li H, Xing MF, 2011. The study on floating hoarfrost in sintered red mud of Zhongzhou aluminum plant. *China Resources Comprehensive Utilization*, 29(6):21-23 (in Chinese).
https://doi.org/10.3969/j.issn.1008-9500.2011.06.003

Youssef NF, Shater MO, Ostrovsky O, et al., 2001. Utilization of red mud in the manufacture of ceramic tiles. *Key Engineering Materials*, 206-213:1775-1778.
https://doi.org/10.4028/www.scientific.net/KEM.206-213.1775

Zhang JZ, Liu SJ, Yao ZY, et al., 2018. Environmental aspects and pavement properties of red mud waste as the replacement of mineral filler in asphalt mixture. *Construction and Building Materials*, 180:605-613.
https://doi.org/10.1016/j.conbuildmat.2018.05.268

Zhang JZ, Yao ZY, Wang K, et al., 2021. Sustainable utilization of bauxite residue (red mud) as a road material in pavements: a critical review. *Construction and Building Materials*, 270:121419.
https://doi.org/10.1016/j.conbuildmat.2020.121419

Zhang LY, 2013. Production of bricks from waste materials–a review. *Construction and Building Materials*, 47:643-655.
https://doi.org/10.1016/j.conbuildmat.2013.05.043

Zhang N, Liu XM, Sun HH, et al., 2011. Pozzolanic behaviour of compound-activated red mud-coal gangue mixture. *Cement and Concrete Research*, 41(3):270-278.
https://doi.org/10.1016/j.cemconres.2010.11.013

Zhao H, Gou HY, 2021. Unfired bricks prepared with red mud and calcium sulfoaluminate cement: properties and environmental impact. *Journal of Building Engineering*, 38:102238.
https://doi.org/10.1016/j.jobe.2021.102238

Zhao Y, Liang NX, Chen H, et al., 2020. Preparation and properties of sintering red mud unburned road brick using orthogonal experiments. *Construction and Building Materials*, 238:117739.
https://doi.org/10.1016/j.conbuildmat.2019.117739

Zhong L, Zhang YF, Zhang Y, 2009. Extraction of alumina and sodium oxide from red mud by a mild hydro-chemical process. *Journal of Hazardous Materials*, 172(2-3):1629-1634.
https://doi.org/10.1016/j.jhazmat.2009.08.036

Zhou LF, Gou MF, Luo SQ, 2021. Hydration kinetics of a calcination activated bauxite tailings-lime-gypsum ternary system. *Journal of Building Engineering*, 38:102189.
https://doi.org/10.1016/j.jobe.2021.102189

Zhou W, Shi XY, Lu X, et al., 2020. The mechanical and microstructural properties of refuse mudstone-GGBS-red mud based geopolymer composites made with sand. *Construction and Building Materials*, 253:119193. https://doi.org/10.1016/j.conbuildmat.2020.119193

Zinoveev D, Grudinsky P, Zakunov A, et al., 2019. Influence of Na_2CO_3 and K_2CO_3 addition on iron grain growth during carbothermic reduction of red mud. *Metals*, 9(12): 1313. https://doi.org/10.3390/met9121313

Introducing Editorial Board Member

Prof. Tung-Chai LING has been the editorial board member of *Journal of Zhejiang University-SCIENCE A (Applied Physics & Engineering)* since 2016. He is a professor at College of Civil Engineering, Hunan University, China. Prior to the appointment, he was worked at the USA, UK, HK SAR of China, and Malaysia, focusing on the resource utilization of solid wastes and carbon sequestration technology in the field of construction materials. His works have been published in 129 SCI journal papers (100 as first/corresponding author), garnering over 4400 citations and an h-index of 41. He presided over 18 competitive national and provincial research projects. He has been elected as an associate fellow of the ASEAN Academy of Engineering and Technology (AAET), and fellow of the Hong Kong Concrete Institute (HKCI), China; serving as the associate editor of the ASCE *Journal of Materials in Civil Engineering* and the editorial board member of several international journals. He has been listed as one of the top 2% of global scientists (Career-long impact), and was awarded the "Robert L'Hermite Medal" by International Union of Laboratories and Experts in Construction Materials, Systems and Structures (RILEM) in 2020. The medal is awarded to one young outstanding scientist globally every year, and he is the first scholar from a Chinese university to receive this prestigious award since the inception of the medal in 1967.